

Durham Research Online

Deposited in DRO:

01 May 2017

Version of attached file:

Accepted Version

Peer-review status of attached file:

Peer-reviewed

Citation for published item:

Baxevanakis, K.P. and Gourgiotis, P.A. and Georgiadis, H.G. (2017) 'Interaction of cracks with dislocations in couple-stress elasticity. Part I : Opening mode.', International journal of solids and structures., 118-119 . pp. 179-191.

Further information on publisher's website:

<https://doi.org/10.1016/j.ijsolstr.2017.03.019>

Publisher's copyright statement:

© 2017 This manuscript version is made available under the CC-BY-NC-ND 4.0 license
<http://creativecommons.org/licenses/by-nc-nd/4.0/>

Additional information:

Use policy

The full-text may be used and/or reproduced, and given to third parties in any format or medium, without prior permission or charge, for personal research or study, educational, or not-for-profit purposes provided that:

- a full bibliographic reference is made to the original source
- a [link](#) is made to the metadata record in DRO
- the full-text is not changed in any way

The full-text must not be sold in any format or medium without the formal permission of the copyright holders.

Please consult the [full DRO policy](#) for further details.

Interaction of cracks with dislocations in couple-stress elasticity.

Part I: Opening mode

K.P. Baxevanakis^{1*}, P.A. Gourgiotis², H.G. Georgiadis^{1**}

¹ *Mechanics Division, National Technical University of Athens, Zographou, GR-15773, Greece*

² *School of Engineering & Computing Sciences, Durham University, South Road, Durham, DH1 3LE, U.K.*

Abstract: In the present work the interaction of a finite-length crack with a discrete climb dislocation is studied within the framework of the generalized continuum theory of couple-stress elasticity. The climb dislocation is placed on the crack plane resulting in an opening crack mode. For the solution of the crack problem the distributed dislocation technique is employed. Due to the nature of the boundary conditions that arise in couple-stress elasticity, the crack is modeled by a continuous distribution of translational and rotational defects. The distribution of these defects produces both stresses and couple stresses in the body. It is shown that the interaction problem is governed by a system of coupled singular integral equations with both Cauchy and logarithmic kernels which is solved numerically using an appropriate collocation technique. The results for the near-tip fields differ in several respects from the predictions of classical fracture mechanics. It is shown that a cracked couple-stress solid behaves in a more rigid way compared to one governed by classical elasticity. Moreover, the evaluation of the energy release rate in the crack-tips and the associated driving force exerted on the dislocation reveals an interesting ‘alternating’ behavior between strengthening and weakening of the crack, depending on the distance of the crack-tip to the dislocation core as well as on ratio of the material length, introduced by the couple-stress theory, to the length of the crack.

Keywords: Cracks; Disclinations; Microstructure; Distributed Dislocation Technique; Peach-Koehler force; couple-stress theory.

* Current affiliation: Theoretical & Applied Mechanics Group, Mechanical Engineering & Mechanics Department, Drexel University, 3141 Chestnut Street, Philadelphia, PA 19104, USA.

** Corresponding author: H.G. Georgiadis. E-mail address: georgiad@central.ntua.gr

1. Introduction

The interaction between a crack and a dislocation is a fundamental problem of fracture mechanics since it determines, in many cases, the macroscopic brittle or ductile material response. Extensive work on this problem is reported in the literature within the framework of classical isotropic and anisotropic elasticity. Rice and Thomson (1974) proposed an energy condition for dislocation emission from a crack-tip discussing the consequent way of fracture, brittle or ductile. Later, Thomson (1978) and Weertman (1978) introduced the idea of a dislocation shielded crack and the concept of the dislocation free zone. In this model, the emitted dislocation is expected to glide away from the crack-tip until the interaction force is balanced by the lattice friction force and the dislocation comes to rest. The distance between the crack-tip and the point that the dislocation comes to rest is termed as dislocation free zone. Moreover, emitted dislocations are known to reduce the stress field in the vicinity of the crack-tip and hence the local stress intensity factor. An additional solution was given by Zhang and Li (1991) who employed the complex potential method to calculate the stress intensity factors at the crack-tips and the image forces due to the presence of a discrete dislocation. Accordingly, Markenscoff (1993) provided a solution for the stress field ahead of the crack-tip using integral equations. On the other hand, there are numerous experimental observations of these phenomena and we may refer indicatively to Kobayashi and Ohr (1981), and Michot and George (1986).

In the present work, the interaction of a finite-length crack with discrete dislocations is studied using the generalized continuum theory of couple-stress elasticity to account for effects induced by the material microstructure. The couple-stress elasticity theory (also known as constrained Cosserat theory) is a particular case of the general approach of Mindlin (1964) and is the simplest theory of elasticity in which couple-stresses are introduced. The fundamental concepts of the couple-stress theory were first presented in rudimentary form by Cosserat and Cosserat (1909), but the subject was generalized and reached maturity in the 1960s through the works of Mindlin and Tiersten (1962), Toupin (1962), and Koiter (1964). Work employing the couple-stress theory in elasticity and plasticity problems has been intensified in recent years (see e.g. Vardoulakis and Sulem, 1995; Georgiadis and Velgaki, 2003; Lubarda, 2003; Park and Gao, 2006; Radi 2008; Bigoni and Gourgiotis, 2016 and references therein) mainly due to the increasing need of predicting accurately the macroscopical behaviour of advanced

microstructured materials (such as ceramics, polymers, foams, and cellular materials) that are extensively used nowadays in many engineering applications.

Regarding crack problems in the framework of couple-stress elasticity, several solutions were contributed to the literature. Confining attention to plane-strain problems, Sternberg and Muki (1967) were the first to study the problem of a finite-length crack under mode I loading by applying the method of dual integral equations. One of the main findings of this investigation was that both stress and couple-stress fields exhibit a square root singularity at the crack-tip, just as in classical elasticity theory. Atkinson and Leppington (1977) studied the problem of a semi-infinite crack with exponentially decaying normal tractions on the crack faces using the Wiener-Hopf technique. Accordingly, Itou (1981) evaluated numerically the stress intensity factor at the crack-tip of a propagating Yoffe crack. Huang et al. (1997) provided the near-tip expressions for mode I and mode II crack problems employing the asymptotic Knein-Williams method. Later, Huang et al. (1999) presented full-field solutions for of semi-infinite crack problems in elastic and elastoplastic materials characterized by couple-stress elasticity. More recently, Gourgiotis and Georgiadis (2007, 2008) extended the distributed dislocation technique (DDT) to study finite-length cracks under constant remote loading while Gourgiotis et al. (2012) investigated the problem of a semi-infinite crack under concentrated shear loading using the Wiener-Hopf technique. Finally, Gourgiotis and Piccolroaz (2014) considered problems of dynamically propagating crack under mode II loading conditions in the framework of couple-stress elasticity.

In light of the previous studies, it is anticipated that the consideration of the material microstructure though the introduction of couple-stresses will alter the near tip solutions of the interaction problem investigated herein. Our approach is based on the DDT to construct the integral equations that describe the crack problems (for a detailed review of the DDT, we refer to the treatise by Hills et al. (1996). As a first approximation, we assume that the defects lie *along* the crack-plane and are not emitted by the crack-tip. In Part I of this work, we study the interaction of a crack with a discrete ‘climb’* dislocation, resulting to a crack opening-mode. The interaction of a crack with a glide and a screw dislocation, resulting to sliding and tearing modes, respectively, is examined in Part II of this work.

* The jargon term ‘climb’ refers to an edge dislocation with its Burgers vector *perpendicular* to the cut made to create the defect in the classic way (Hills et al., 1996).

Following the approach employed in similar cases, the solution to the problem is obtained by the superposition of solutions of two auxiliary problems: an *un-cracked* medium (of the same geometry) subjected to the field of a climb dislocation and a *cracked* body loaded along the crack faces by equal and opposite tractions to those generated in the first auxiliary problem (corrective solution). Contrary to the classical elasticity case, in order to satisfy the boundary conditions of the second auxiliary problem, it is necessary to distribute *both* translational and rotational defects along the crack faces (see e.g. Gourgiotis and Georgiadis, 2008). This rotational defect was termed by the latter authors as ‘constrained’ wedge disclination and, in fact, corresponds to crystal twinning. The continuous distribution of these discontinuities along the crack faces results in a *coupled* system of singular integral equations with Cauchy and logarithmic kernels which is solved numerically using an appropriate collocation technique. Of particular interest is the evaluation of the energy release rate in both crack-tips (*J*-integral) as well as the calculation of the driving force exerted on the discrete edge dislocation. The comparison of these quantities in the framework of couple-stress elasticity with the classical elasticity solutions (which are also obtained in closed form herein) reveals an interesting ‘alternating’ behavior between strengthening and weakening effects depending on the distance of the discrete climb dislocation from the crack-tip and the magnitude of the characteristic material length with respect to the length of the crack.

2. Basic equations of couple-stress elasticity in plane strain

The general idea in the so-called generalized continuum theories (one of which is the couple-stress theory) is considering a continuum with material particles (macro-volumes), behaving like *deformable* bodies (Mindlin, 1964). This behavior can easily be realized if such a material particle is viewed as a collection of sub-particles. It is further assumed that internal forces (called dipolar or double forces) are developed between the sub-particles. Although each pair of the dipolar forces has a zero resultant force, it generally produces a *non-zero* moment and therefore gives rise to stresses on a surface called couple-stresses. This means that a surface element may transmit, besides the usual force vector, a *couple* vector as well. One can interpret physically the couple-stresses as created by frictional couples resisting the relative rotation of the grains (sub-particles). The basic concepts of linear couple-stress elasticity have been well documented in the fundamental papers of Mindlin and Tiersten (1962) and Koiter (1964).

In this section, we briefly summarize the basic equations in the plane strain case under static loading conditions. For a body that occupies a domain in the (x, y) -plane, the two-dimensional displacement field is described by

$$u_x \equiv u_x(x, y) \neq 0, \quad u_y \equiv u_y(x, y) \neq 0, \quad u_z \equiv 0, \quad (1)$$

where the z axis is perpendicular to the (x, y) -plane.

Regarding, the kinematical description of the elastic body, the non-vanishing components of the strain tensor, the rotation vector, and the curvature tensor are given as follows

$$\begin{aligned} \varepsilon_{xx} &= \frac{\partial u_x}{\partial x}, \quad \varepsilon_{yy} = \frac{\partial u_y}{\partial y}, \quad \varepsilon_{xy} = \varepsilon_{yx} = \frac{1}{2} \left(\frac{\partial u_x}{\partial y} + \frac{\partial u_y}{\partial x} \right), \\ \omega_z &\equiv \omega = \frac{1}{2} \left(\frac{\partial u_y}{\partial x} - \frac{\partial u_x}{\partial y} \right), \quad \kappa_{xz} = \frac{\partial \omega}{\partial x}, \quad \kappa_{yz} = \frac{\partial \omega}{\partial y} \end{aligned} \quad (2)$$

Further, the equations of force and moment equilibrium in the absence of body forces and body couples reduce to

$$\frac{\partial \sigma_{xx}}{\partial x} + \frac{\partial \sigma_{yx}}{\partial y} = 0, \quad \frac{\partial \sigma_{xy}}{\partial x} + \frac{\partial \sigma_{yy}}{\partial y} = 0, \quad \sigma_{xy} - \sigma_{yx} + \frac{\partial m_{xz}}{\partial x} + \frac{\partial m_{yz}}{\partial y} = 0, \quad (3)$$

where σ_{pq} and μ_{pq} are the components of the stress tensor and couple-stress tensor (both being asymmetric).

Assuming a linear and isotropic material response the strain energy density takes the following form

$$W = (\lambda/2) (\varepsilon_{xx} + \varepsilon_{yy})^2 + \mu (\varepsilon_{xx}^2 + 2\varepsilon_{xy}^2 + \varepsilon_{yy}^2) + 2\mu\ell^2 (\kappa_{xz}^2 + \kappa_{yz}^2). \quad (4)$$

where λ and μ are Lamé type constants, ν is the Poisson's ratio, and ℓ is the characteristic material length introduced in couple-stress elasticity.

Accordingly, the constitutive equations in the plane-strain case become

$$\begin{aligned}\varepsilon_{xx} &= (2\mu)^{-1} \left[\sigma_{xx} - \nu(\sigma_{xx} + \sigma_{yy}) \right], \quad \varepsilon_{yy} = (2\mu)^{-1} \left[\sigma_{yy} - \nu(\sigma_{xx} + \sigma_{yy}) \right], \\ \varepsilon_{xy} &= (4\mu)^{-1} (\sigma_{xy} + \sigma_{yx}),\end{aligned}\tag{5}$$

and

$$\kappa_{xz} = (4\mu\ell^2)^{-1} m_{xz}, \quad \kappa_{yz} = (4\mu\ell^2)^{-1} m_{yz}.\tag{6}$$

In view of the above, the non-vanishing components of the stress tensor can be expressed in terms of the displacement components as

$$\sigma_{xx} = (\lambda + 2\mu) \frac{\partial u_x}{\partial x} + \lambda \frac{\partial u_y}{\partial y},\tag{7}$$

$$\sigma_{yy} = (\lambda + 2\mu) \frac{\partial u_y}{\partial y} + \lambda \frac{\partial u_x}{\partial x},\tag{8}$$

$$\sigma_{yx} = \mu \left(\frac{\partial u_x}{\partial y} + \frac{\partial u_y}{\partial x} \right) + \mu\ell^2 \left(\frac{\partial^3 u_y}{\partial x^3} - \frac{\partial^3 u_x}{\partial x^2 \partial y} + \frac{\partial^3 u_y}{\partial x \partial y^2} - \frac{\partial^3 u_x}{\partial y^3} \right),\tag{9}$$

$$\sigma_{xy} = \mu \left(\frac{\partial u_x}{\partial y} + \frac{\partial u_y}{\partial x} \right) - \mu\ell^2 \left(\frac{\partial^3 u_y}{\partial x^3} - \frac{\partial^3 u_x}{\partial x^2 \partial y} + \frac{\partial^3 u_y}{\partial x \partial y^2} - \frac{\partial^3 u_x}{\partial y^3} \right).\tag{10}$$

Finally, combining the equilibrium equations (3) with (7)-(10), we obtain the following system of coupled partial differential equations of the fourth order in terms of the components of the two dimensional displacement field

$$\frac{1}{1-2\nu} \frac{\partial}{\partial x} \left[2(1-\nu) \frac{\partial u_x}{\partial x} + \frac{\partial u_y}{\partial y} \right] + \frac{\partial^2 u_x}{\partial y^2} + \ell^2 \left(\frac{\partial^4 u_y}{\partial x^3 \partial y} - \frac{\partial^4 u_x}{\partial x^2 \partial y^2} + \frac{\partial^4 u_y}{\partial x \partial y^3} - \frac{\partial^4 u_x}{\partial y^4} \right) = 0, \tag{11}$$

$$\frac{1}{1-2\nu} \frac{\partial}{\partial y} \left[2(1-\nu) \frac{\partial u_y}{\partial y} + \frac{\partial u_x}{\partial x} \right] + \frac{\partial^2 u_y}{\partial x^2} + \ell^2 \left(\frac{\partial^4 u_x}{\partial x^3 \partial y} - \frac{\partial^4 u_y}{\partial x^2 \partial y^2} + \frac{\partial^4 u_x}{\partial x \partial y^3} - \frac{\partial^4 u_y}{\partial x^4} \right) = 0. \quad (12)$$

3. Formulation of the crack problem

Consider a straight crack of finite length $2a$ in an infinite couple-stress elastic medium and a discrete ‘climb’ dislocation of Burgers vector $\mathbf{b} = (0, b_y, 0)$ lying at the crack-plane ($y = 0$) at a distance d ($d > a$) from the center of the crack (Fig. 1). No other loading is applied to the body. The crack faces are described by the unit vector $\mathbf{n} = (0, \pm 1)$ and assumed to be traction-free. The boundary conditions along the crack faces assume then the following form

$$\sigma_{yy}(x, 0) = 0, \quad \sigma_{yx}(x, 0) = 0, \quad m_{yz}(x, 0) = 0, \quad \text{for } |x| < a, \quad (13)$$

which are supplemented by the regularity conditions at infinity

$$\sigma_{pq}^\infty \rightarrow 0, \quad m_{qz}^\infty \rightarrow 0, \quad \text{as } r \rightarrow \infty, \quad (14)$$

where $(p, q) = (x, y)$ and $r = (x^2 + y^2)^{1/2}$ is the distance from the origin. Equation (14) suggests that there is no external loading induced other than the one induced by the discrete climb dislocation.

As it is shown in Gourgiotis and Georgiadis (2008), a discrete climb dislocation in an *infinite* isotropic couple-stress medium induces *both* normal stresses $\sigma_{yy}^{(b_y)}(x, 0)$ and couple-stresses $m_{yz}^{(b_y)}(x, 0)$ along the slip plane $y = 0$. However, a climb dislocation does not induce shear stresses at $y = 0$, so that $\sigma_{yx}^{(b_y)}(x, 0) = 0$. The stress field for a discrete climb dislocation in couple-stress elasticity has been analytically derived in Gourgiotis and Georgiadis (2008). An outline of the procedure is provided in Section 4 (c.f. Eqs (19) and (20)) and in Appendix A.

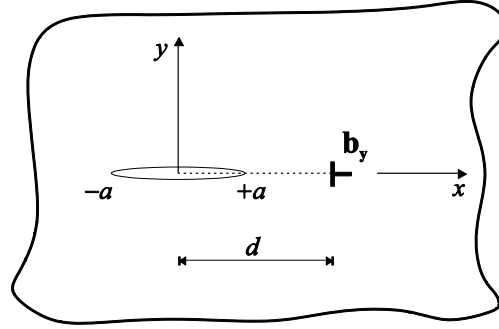


Fig. 1: Interaction of a finite length crack with a discrete climb dislocation placed along the crack-plane at a distance d from the center of the crack.

The solution to the main crack problem can be derived by superposing the solutions of two auxiliary problems. First, we consider an *un-cracked* body subjected to the loading of a discrete climb dislocation placed along the crack line ($y=0$) and at a distance d from the crack center (origin of the axes). Next, for the second auxiliary problem (referred often as *corrective solution*), a body of identical geometry with the initial *cracked* body without the discrete climb dislocation is considered. The only loading is applied along the crack faces consisting of equal and opposite tractions to those generated in the first auxiliary problem (*un-cracked* body). The boundary conditions along the crack-faces ($|x| < a$) assume then the following form

$$\sigma_{yy}(x, 0) = -\sigma_{yy}^{(b_y)}(x-d, 0), \quad \sigma_{yx}(x, 0) = 0, \quad m_{yz}(x, 0) = -m_{yz}^{(b_y)}(x-d, 0). \quad (15)$$

It is remarked that the same boundary value problem in the framework of classical isotropic elasticity is described by only the first two conditions in Eqs (15). In that case, a distribution of climb dislocations along the crack faces would be sufficient to solve the respective mode I problem (Hills et al. 1996). However, in couple-stress theory, it is not possible to satisfy simultaneously the three boundary conditions in Eq. (15) solely by distributing climb dislocations. Indeed, as already shown in Gourgiotis and Georgiadis (2008), the boundary conditions are satisfied by distributing *both* translational and rotational defects since the work

conjugates of the force traction $P_y = \sigma_{yy} n_y$ and the tangential couple traction $R_z = m_{yz} n_y$ are the displacement u_y and the rotation ω , respectively (Mindlin and Tiersten, 1962; Koiter, 1964).

In the next section, we derive the stress fields of the two defects that will serve as influence functions for the opening mode crack problem under consideration.

4. Influence functions for the opening mode crack problem

The influence functions for the opening mode crack problem in couple-stress elasticity have been obtained in Gourgiotis and Georgiadis (2008). In this section, for the sake of completeness, we will briefly summarize their derivation procedure and cite the results pertinent to our analysis. As it was discussed in the previous section, both translational and rotational defects must be distributed along the crack-faces to render the crack traction-free. To this purpose, the stress and couple-stress fields of a climb dislocation and of the appropriate rotational defect in infinite isotropic space will be obtained by solving the appropriate boundary value problems.

Due to symmetry only the upper half plane $(-\infty < x < \infty, y \geq 0)$ is considered. The boundary value problems for the two defects in couple-stress elasticity take then the following form:

Climb dislocation:

$$u_y(x, 0^+) = -\frac{b_y}{2} H(x), \quad \omega(x, 0^+) = 0, \quad \sigma_{yx}(x, 0^+) = 0, \quad (16)$$

Constrained wedge disclination:

$$u_y(x, 0^+) = 0, \quad \omega(x, 0^+) = \frac{\Omega}{2} H(x), \quad \sigma_{yx}(x, 0^+) = 0, \quad (17)$$

where $H(x)$ is the Heaviside step function. Equations (17) describe the problem of a “constrained” wedge disclination with Frank vector $\Omega = (0, 0, \Omega)$ in an infinite couple-stress material. The term constrained wedge disclination was introduced by Gourgiotis and Georgiadis

(2008) and is justified by the fact that the discontinuity in the rotation vector does not affect the normal displacement u_y as opposed to the standard wedge disclination in classical elasticity theory (see e.g. deWit, 1973) or in couple-stress elasticity (Anthony, 1970). Indeed, in these cases, the discontinuity in the rotation vector introduces also a discontinuity in the normal displacement at the disclination plane ($y=0$) given by the expression: $u_y(x, 0^+) = (\Omega/2)xH(x)$ (Fig. 2a). Moreover, the stresses introduced by a standard wedge disclination become logarithmically unbounded at infinity. Thus, the standard wedge disclination cannot be used to generate a traction free crack in the framework of couple-stress elasticity.

In Mechanics of Defects, the rotational defect referred to as constrained wedge disclination corresponds to crystal twinning (Fig. 2b). This phenomenon occurs during crystal growth or under certain stress or temperature conditions and describes the formation of two or more intergrown crystals that share some of the same crystal lattice points in a symmetrical manner (denoted as ‘twinning plane’ in Fig. 2b). This procedure is more prominent in lower symmetry (e.g. hexagonal close packed) crystals where twins need to undertake part of the crystal’s plastic deformation in order to fulfill Taylor’s condition for five independent slip systems (see e.g. Christian and Mahajan, 1995).

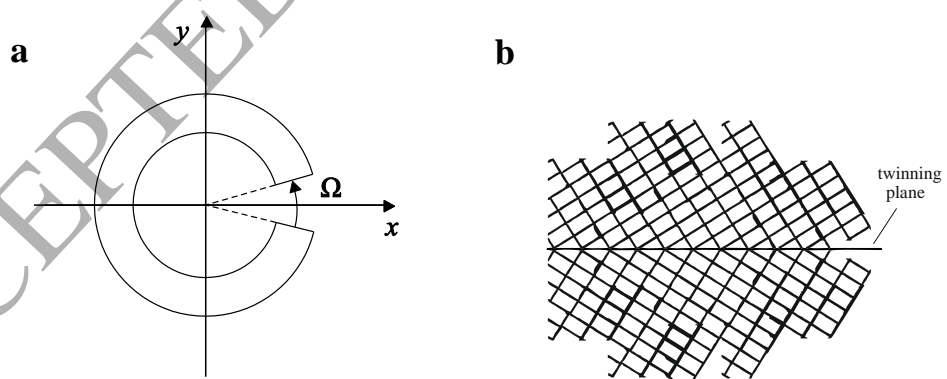


Fig. 2: (a) Standard wedge disclination with Frank vector $\Omega = (0, 0, \Omega)$,
(b) twinning of two tetragonal twin crystals.

The two boundary value problems are attacked using the Fourier integral transform method in order to eliminate the x -dependence in the field equations (11)-(12) and the boundary conditions (16)-(17) (details of the procedure are provided in Appendix A). The influence functions, corresponding to the normal stress σ_{yy} and the couple-stress m_{yz} along the crack line $y = 0$, are derived from the superposition of the two defects. These are given as

$$\sigma_{yy}(x, 0) = \sigma_{yy}^{(b_y)}(x, 0) + \sigma_{yy}^{(\Omega)}(x, 0), \quad m_{yz}(x, 0) = m_{yz}^{(b_y)}(x, 0) + m_{yz}^{(\Omega)}(x, 0), \quad (18)$$

where

$$\begin{cases} \sigma_{yy}^{(b_y)}(x, 0) = b_y L_{11}(x), & m_{yz}^{(b_y)}(x, 0) = b_y L_{12}(x) \\ \sigma_{yy}^{(\Omega)}(x, 0) = \Omega L_{12}(x), & m_{yz}^{(\Omega)}(x, 0) = \Omega L_{22}(x) \end{cases}, \quad (19)$$

and

$$\begin{cases} L_{11}(x) = \frac{\mu}{2\pi(1-\nu)x} + \frac{2\mu}{\pi x} \left[\frac{2\ell^2}{x^2} - K_2\left(\frac{|x|}{\ell}\right) \right] \\ L_{12}(x) = \frac{\mu}{\pi} \left[K_2\left(\frac{|x|}{\ell}\right) - \frac{2\ell^2}{x^2} \right] - \frac{\mu}{\pi} K_0\left(\frac{|x|}{\ell}\right) \\ L_{22}(x) = \frac{\mu\ell}{2\pi} \operatorname{sgn}(x) G_{1,3}^{2,1} \left(\frac{x^2}{4\ell^2} \middle| \begin{matrix} 1 \\ -1/2, 1/2, 0 \end{matrix} \right) \end{cases}. \quad (20)$$

Note that $K_i(\cdot)$ is the i^{th} order modified Bessel function of the second kind and $G_{c,d}^{a,b}(\cdot)$ is the MeijerG (see e.g. Erdélyi et al., 1953).

Regarding the characteristics of the stress field described above, the following points are of notice:

(i) As $x \rightarrow 0$, the modified Bessel functions and the MeijerG function have the following asymptotic behavior

$$K_2(|x|) = 2x^{-2} - 1/2 + O(x^2 \ln|x|), \quad K_0(|x|) = O(-\ln|x|),$$

$$G_{1,3}^{2,1} \left(x^2 \Big|_{-1/2, 1/2, 0}^1 \right) = O(2|x|^{-1}). \quad (21)$$

Based on the above asymptotic relations, it can be readily inferred that the normal stress σ_{yy} in (18)₁ exhibits, as $x \rightarrow 0$, a *Cauchy* type singularity due to the climb dislocation and a *logarithmic* singularity due to the constrained wedge disclination. On the other hand, the couple-stress m_{yz} in (18)₂ has a *Cauchy* type singularity due to the constrained wedge disclination and a *logarithmic* singularity due to the climb dislocation.

(ii) As $x \rightarrow \pm\infty$, it can be derived that $\sigma_{yy} \rightarrow 0$ whereas $m_{yz} \rightarrow \mp \mu \ell \Omega$. Thus, the constrained wedge disclination does not induce normal stresses at infinity contrary to the standard wedge disclination where the stress becomes logarithmically unbounded both in classical and in couple-stress elasticity.

(iii) As $\ell \rightarrow 0$, the couple-stress m_{yz} vanishes, that is, the constrained wedge disclination induces stresses and couple-stresses only when the material microstructure is considered ($\ell > 0$). Moreover, for $\ell \rightarrow 0$, the normal stress σ_{yy} reduces to the respective one of classical elasticity in the case of a discrete climb dislocation. In the latter case, the normal stress is given by the relation $\sigma_{yy} = \mu b_y / 2\pi(1-\nu)x$, which is the influence function of the classical mode-I crack problem (Hills et al. 1996).

5. Singular integral equation approach

The discrete defects examined in the previous Section have to be distributed along the crack faces so that the corrective stresses of Eq. (15) are generated. The elastic field produced by the continuous distributions of climb dislocations and constrained wedge disclinations is derived by integrating the governing equations (19) and (20) along the crack faces. Note that the second boundary condition in Eqs. (15) is automatically satisfied since none of these defects induces shear stresses at the crack plane $y = 0$. Eventually, the simultaneous satisfaction of the first and

third boundary conditions in Eq. (15) leads to a system of coupled integral equations. Employing asymptotic analysis, we separate the singular from the regular parts of the kernels and obtain the following system singular integral equations

$$\begin{aligned} -\sigma_{yy}^{(b_y)}(x-d,0) = & \frac{\mu(3-2\nu)}{2\pi(1-\nu)} \int_{-a}^a \frac{B_l(t)}{x-t} dt + \frac{\mu}{\pi a} \int_{-a}^a W(t) \ln \frac{|x-t|}{\ell} dt \\ & + \frac{2\mu}{\pi} \int_{-a}^a B_l(t) R_1(x-t) dt - \frac{\mu}{\pi a} \int_{-a}^a W(t) R_2(x-t) dt, \quad |x| < a, \end{aligned} \quad (22)$$

$$\begin{aligned} -m_{yz}^{(b_y)}(x-d,0) = & -\frac{2\mu\ell^2}{\pi a} \int_{-a}^a \frac{W(t)}{x-t} dt + \frac{\mu}{\pi} \int_{-a}^a B_l(t) \ln \frac{|x-t|}{\ell} dt \\ & - \frac{\mu}{\pi} \int_{-a}^a B_l(t) R_2(x-t) d\xi + \frac{\mu\ell}{2\pi a} \int_{-a}^a W(t) R_3(x-t) dt, \quad |x| < a, \end{aligned} \quad (23)$$

where the quantities $B_l(t)$ and $W(t)$ are the densities of the climb dislocation and the constrained wedge disclination respectively, defined as

$$B_l(t) = \frac{db_y(t)}{dt} = -\frac{d\Delta u_y(t)}{dt}, \quad \Delta u_y(x) = -\int_{-a}^x B_l(t) dt. \quad (24)$$

$$W(t) = a \frac{d\Omega(t)}{dt} = a \frac{d\Delta\omega(t)}{dt}, \quad \Delta\omega(x) = \frac{1}{a} \int_{-a}^x W(t) dt. \quad (25)$$

In the above expressions, $\Delta u_y(x)$ is the relative opening displacement and $\Delta\omega(x)$ the relative rotation between the upper and lower crack faces. The climb dislocation density can be interpreted as the negative of the slope whereas the constrained disclination density as the curvature at a point on the crack faces. It should be also noted that both densities are dimensionless. The expressions for the normal stress $\sigma_{yy}^{(b_y)}$ and the couple-stress $m_{yz}^{(b_y)}$ appearing on the LHS of (22) and (23) are given in Eq. (19)₁.

Moreover, the kernels $R_q(x-t)$ with $q=1, 2, 3$, read

$$\begin{aligned}
 R_1(x-t) &= \frac{1}{x-t} \left[\frac{2\ell^2}{(x-t)^2} - K_2\left(\frac{|x-t|}{\ell}\right) - \frac{1}{2} \right], \\
 R_2(x-t) &= \left[\frac{2\ell^2}{(x-t)^2} - K_2\left(\frac{|x-t|}{\ell}\right) \right] + \left[K_0\left(\frac{|x-t|}{\ell}\right) + \ln\left(\frac{|x-t|}{\ell}\right) \right], \\
 R_3(x-t) &= \operatorname{sgn}(x-t) \cdot G_{1,3}^{2,1} \left(\frac{(x-t)^2}{4\ell^2} \middle| \begin{matrix} 1 \\ -1/2, 1/2, 0 \end{matrix} \right) + \frac{4\ell}{x-t}.
 \end{aligned} \tag{26}$$

Employing the asymptotic properties of the modified Bessel functions and the MeijerG function in Eqs (21), it can be shown that the above kernels are *regular* as $x \rightarrow t$.

In addition to the governing equations of the problem, the following closure conditions must be satisfied in order to ensure that the normal displacement and the rotation are single-valued

$$\int_{-a}^a B_I(t) dt = 0, \quad \int_{-a}^a W(t) dt = 0. \tag{27}$$

In the special case that the discrete dislocation lies at the crack-tip, the LHS of Eqs (22) and (23) tends to zero and the contribution of the defect is described by letting the first of (27) be equal to the Burgers vector b_y of the discrete climb dislocation (Markenscoff, 1993). This configuration corresponds to a crack partially filled with a rigid wedge (Barenblatt, 1962).

Regarding the influence of the characteristic length ℓ on the governing equations of the problem, two extreme cases are worth investigating. First, assuming $\ell \rightarrow 0$, it is readily shown that the integral equation (23) vanishes identically while Eq. (22) is reduced to the corresponding equation of classical elasticity, written as (Markenscoff, 1993)

$$\frac{1}{x-d} = \int_{-a}^a \frac{B_I(t)}{x-t} dt, \quad |x| < a. \tag{28}$$

Next, let us consider the limit $\ell \rightarrow \infty$. Multiplying Eq. (23) with ℓ^{-2} and noting that

$$\lim_{\ell \rightarrow \infty} \frac{1}{\ell^2} \ln \frac{|x-t|}{\ell} = 0, \quad \lim_{\ell \rightarrow \infty} \frac{1}{\ell^2} R_2(x-t) = 0, \quad \lim_{\ell \rightarrow \infty} \frac{1}{\ell} R_3(x-t) = 0, \quad (29)$$

the system of singular integral equations (22) and (23) becomes uncoupled. Observing further that $\lim_{\ell \rightarrow \infty} R_1(x-t) = 0$, the integral equation (22) becomes finally

$$\frac{\mu(3-2\nu)}{2\pi(1-\nu)(x-d)} = \frac{\mu(3-2\nu)}{2\pi(1-\nu)} \int_{-a}^a \frac{B_I(t)}{x-t} dt, \quad |x| < a, \quad (30)$$

which is the same integral equation that occurs in classical isotropic elasticity (c.f. Eq. (28)).

We now proceed to the solution of the system of singular integral equations (22) and (23). First, the unknown defect densities, $B_I(t)$ and $W(t)$, should be expressed in such a way to account for the asymptotic behavior of the displacement and rotation at the crack-tips. In couple-stress theory, Sternberg and Muki (1967) and later Huang et al. (1997) showed that both the displacement u_y and the rotation ω behave as $R^{1/2}$ near the crack-tips, where R is now the radial distance from the crack-tip. This asymptotic behavior was verified by the uniqueness theorem for crack problems in couple-stress theory (Grentzelou and Georgiadis, 2005), which suggests that both the displacement and the rotation have to be bounded near the crack-tip region. Taking into account the asymptotic behavior of the defect densities near the crack-tips and utilizing the dimensionless quantities: $\tilde{x} = x/a$, $\tilde{t} = t/a$, and $\tilde{d} = d/a$, we express the densities $B_I(\tilde{t})$ and $W(\tilde{t})$ in the following form

$$B_I(\tilde{t}) = \sum_{n=0}^{\infty} b_n T_n(\tilde{t}) (1-\tilde{t}^2)^{-1/2}, \quad W(\tilde{t}) = \sum_{n=0}^{\infty} c_n T_n(\tilde{t}) (1-\tilde{t}^2)^{-1/2}, \quad |\tilde{t}| < 1, \quad (31)$$

where $T_n(\tilde{t})$ are the Chebyshev polynomials of the first kind (see e.g. Abramowitz and Stegun, 1964), and (b_n, c_n) are unknown parameters (constants). After appropriate normalization over the interval $[-1, 1]$, the system is written as

$$\begin{aligned}
 -\frac{\pi\sigma_{yy}^{(b_y)}(a\tilde{x}-a\tilde{d},0)}{\mu} &= \frac{(3-2\nu)}{2(1-\nu)} \sum_{n=0}^{\infty} b_n \int_{-1}^1 \frac{T_n(\tilde{t})(1-\tilde{t}^2)^{-1/2}}{\tilde{x}-\tilde{t}} d\tilde{t} \\
 &+ \sum_{n=0}^{\infty} c_n \int_{-1}^1 T_n(\tilde{t})(1-\tilde{t}^2)^{-1/2} \ln\left(\frac{a}{\ell}|\tilde{x}-\tilde{t}|\right) d\tilde{t} \\
 &+ 2\sum_{n=0}^{\infty} b_n Q_n^{(1)}(\tilde{x}) - \sum_{n=0}^{\infty} c_n Q_n^{(2)}(\tilde{x}), \quad |\tilde{x}| < 1,
 \end{aligned} \tag{32}$$

$$\begin{aligned}
 -\frac{\pi m_{yz}^{(b_y)}(a\tilde{x}-a\tilde{d},0)}{\mu} &= -\frac{2\ell^2}{a^2} \sum_{n=0}^{\infty} c_n \int_{-1}^1 \frac{T_n(\tilde{t})(1-\tilde{t}^2)^{-1/2}}{\tilde{x}-\tilde{t}} d\tilde{t} \\
 &+ \sum_{n=0}^{\infty} b_n \int_{-1}^1 T_n(\tilde{t})(1-\tilde{t}^2)^{-1/2} \ln\left(\frac{a}{\ell}|\tilde{x}-\tilde{t}|\right) d\tilde{t} \\
 &- \sum_{n=0}^{\infty} b_n Q_n^{(2)}(\tilde{x}) + \frac{\ell}{2a} \sum_{n=0}^{\infty} c_n Q_n^{(3)}(\tilde{x}), \quad |\tilde{x}| < 1,
 \end{aligned} \tag{33}$$

where the functions $Q_n^{(s)}(\tilde{x})$ are defined as

$$Q_n^{(s)}(\tilde{x}) = \int_{-1}^1 T_n(\tilde{t})(1-\tilde{t}^2)^{-1/2} R_s(a\tilde{x}-a\tilde{t}) d\tilde{t}, \quad s=1, 2, 3. \tag{34}$$

The integrals in Eq. (34) are regular and are evaluated using the standard Gauss-Chebyshev quadrature while the singular and weakly singular (logarithmic) integrals in Eq. (32) and (33) are calculated in closed form in Appendix B using Eqs (B1) and (B2), respectively. Moreover, employing the auxiliary conditions (27) it can be readily shown that the constants b_0 and c_0 are equal to zero.

In light of the above, the system of integral equations assumes the following discretized form for $|\tilde{x}| < 1$

$$\begin{aligned}
 -\frac{\sigma_{yy}^{(b_y)}(a\tilde{x}-a\tilde{d},0)}{\mu} &= -\frac{(3-2\nu)}{2(1-\nu)} \sum_{n=1}^{\infty} b_n U_{n-1}(\tilde{x}) - \sum_{n=1}^{\infty} \frac{c_n T_n(\tilde{x})}{n} \\
 &+ 2\sum_{n=1}^{\infty} b_n Q_n^{(1)}(\tilde{x}) - \sum_{n=1}^{\infty} c_n Q_n^{(2)}(\tilde{x})
 \end{aligned} \tag{35}$$

$$-\frac{m_{yz}^{(b_y)}(a\tilde{x}-a\tilde{d},0)}{\mu} = \frac{2\ell^2}{a^2} \sum_{n=1}^{\infty} c_n U_{n-1}(\tilde{x}) - \sum_{n=1}^{\infty} \frac{b_n T_n(\tilde{x})}{n} - \sum_{n=1}^{\infty} b_n Q_n^{(2)}(\tilde{x}) + \frac{\ell}{2a} \sum_{n=1}^{\infty} c_n Q_n^{(3)}(\tilde{x}) \quad (36)$$

The system of algebraic equations (35) and (36) is solved numerically by truncating the series at $n = N$ and using an appropriate collocation technique, where the collocation points are chosen as the roots of the first kind Chebyshev polynomial $U_N(\tilde{x})$, viz. $\tilde{x}_j = \cos(j\pi/(N+1))$ with $j = 1, 2, \dots, N$. Equations (35) and (36) form then an algebraic system of $2N$ equations with $2N$ unknowns. Solution convergence was accomplished for different number of collocation points depending on the ratio ℓ/a as shown in Table 1 (Section 7). After calculating the parameters b_n and c_n ($n = 1, \dots, N$), the densities of the two defects can be evaluated employing Eq. (31). Finally, it should be noted that the numerical scheme employed herein differs from the one utilized in Gourgiotis and Georgiadis (2008).

6. Energy release rate and the Peach-Koehler force

In this Section, we derive the expressions for the energy release rate (J -integral) at the crack-tip and the Peach-Koehler force exerted on the climb dislocation and examine their dependence upon the material and geometrical length scales of the problem. In the framework of couple-stress theory, the energy release rate (ERR) was derived first by Atkinson and Leppington (1974) and proved to be path independent (see also Atkinson and Leppington, 1977; Lubarda and Markenscoff, 2000). For the plane strain case, the J -integral takes the following simple form (Gourgiotis and Georgiadis, 2008)

$$J = \int_C W dy - \left[\sigma_{yy} \frac{\partial u_y}{\partial x} + \sigma_{yx} \frac{\partial u_x}{\partial x} + m_{yz} \frac{\partial \omega}{\partial x} \right] dC, \quad (37)$$

where C is a piecewise smooth contour that surrounds the crack-tip and W is the strain energy density. A convenient contour for the evaluation of the J -integral is a rectangular shaped integration path with vanishing height along the y -direction that surrounds the (left or right) crack-tip as $\varepsilon \rightarrow +0$ (Fig. 3). This concept was first introduced by Freund (1972) to calculate the energy flux during dynamic crack propagation and has thereafter been used to compute energy quantities in the vicinity of crack-tips (see e.g. Burridge, 1976; Georgiadis, 2003; Gourgiotis and Georgiadis, 2008, 2009; Gourgiotis and Piccolroaz, 2014). The benefit of this approach is that only the asymptotic near tip stress and displacement fields suffice for the evaluation of the J -integral. Note that the term $\int_C W dy$ in Eq. (37) vanishes as the height of the rectangular contour tends to zero. Furthermore, taking into account that the shear stress σ_{yx} is zero along the crack plane ($y = 0$), the J -integral (for the right or left crack-tip) may be written as

$$J = -2 \lim_{\varepsilon \rightarrow +0} \left\{ \int_{\pm a - \varepsilon}^{\pm a + \varepsilon} \left[\sigma_{yy}(x, 0^+) \frac{\partial u_y(x, 0^+)}{\partial x} + m_{yz}(x, 0^+) \frac{\partial \omega(x, 0^+)}{\partial x} \right] dx \right\}. \quad (38)$$

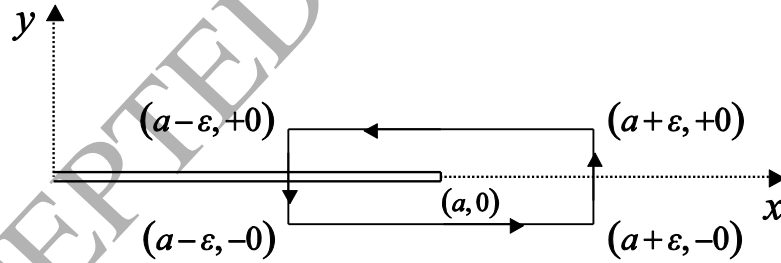


Fig. 3: Rectangular shaped contour for the calculation of J -integral around the right crack-tip.

It should be noted that the dominant near-tip behavior of the normal stress σ_{yy} and the couple-stress m_{yz} is attributed to the Cauchy type integrals in Eqs (22) and (23), respectively. The

asymptotic behavior of these stresses near the right ($x \rightarrow a^+$) and left ($x \rightarrow -a^-$) crack-tips is given as (see Eq. (B3) in Appendix B)

$$\begin{cases} \sigma_{yy}(x \rightarrow a^+, 0^+) = \frac{\mu(3-2\nu)}{2\sqrt{2}(1-\nu)} \sum_{n=1}^N b_n (\tilde{x}-1)^{-1/2} \\ \sigma_{yy}(x \rightarrow -a^-, 0^+) = -\frac{\mu(3-2\nu)}{2\sqrt{2}(1-\nu)} \sum_{n=1}^N (-1)^n b_n |\tilde{x}+1|^{-1/2} \end{cases}, \quad |\tilde{x}| > 1, \quad (39)$$

$$\begin{cases} m_{yz}(x \rightarrow a^+, 0^+) = -\frac{\sqrt{2}\mu\ell^2}{a} \sum_{n=1}^N c_n (\tilde{x}-1)^{-1/2} \\ m_{yz}(x \rightarrow -a^-, 0^+) = \frac{\sqrt{2}\mu\ell^2}{a} \sum_{n=1}^N (-1)^n c_n |\tilde{x}+1|^{-1/2} \end{cases}, \quad |\tilde{x}| > 1. \quad (40)$$

Moreover, in view of the definitions (24) and (25), the following asymptotic relations hold for the gradients of the displacement and rotation

$$\begin{cases} \frac{\partial u_y(x \rightarrow a^-, 0^+)}{\partial x} = -\frac{1}{2\sqrt{2}} \sum_{n=1}^N b_n (1-\tilde{x})^{-1/2} \\ \frac{\partial u_y(x \rightarrow -a^+, 0^+)}{\partial x} = -\frac{1}{2\sqrt{2}} \sum_{n=1}^N (-1)^n b_n (1+\tilde{x})^{-1/2} \end{cases}, \quad |\tilde{x}| < 1, \quad (41)$$

$$\begin{cases} \frac{\partial \omega(x \rightarrow a^-, 0^+)}{\partial x} = \frac{1}{2\sqrt{2}a} \sum_{n=1}^N c_n (1-\tilde{x})^{-1/2} \\ \frac{\partial \omega(x \rightarrow -a^+, 0^+)}{\partial x} = \frac{1}{2\sqrt{2}a} \sum_{n=1}^N (-1)^n c_n (1+\tilde{x})^{-1/2} \end{cases}, \quad |\tilde{x}| < 1. \quad (42)$$

Based on the previous results, the J -integral for the right crack-tip is written in the form

$$\begin{aligned}
 J_r &= -2a \lim_{\varepsilon \rightarrow 0} \left\{ -\frac{\mu}{2} \left[\Lambda_1^{(r)} + \left(\frac{\ell}{a} \right)^2 \Lambda_2^{(r)} \right] \cdot \int_{-\varepsilon/a}^{\varepsilon/a} (x_+)^{-1/2} \cdot (x_-)^{-1/2} d\bar{x} \right\} \\
 &= \frac{\mu\pi a}{2} \left[\Lambda_1^{(r)} + \left(\frac{\ell}{a} \right)^2 \Lambda_2^{(r)} \right],
 \end{aligned} \tag{43}$$

where

$$\Lambda_1^{(r)} = \frac{(3-2\nu)}{4(1-\nu)} \left(\sum_{n=1}^N b_n \right)^2, \quad \Lambda_2^{(r)} = \left(\sum_{n=1}^N c_n \right)^2, \tag{44}$$

and $\bar{x} = \tilde{x} - 1$. Note that for any real number λ , excluding the values $\lambda = -1, -2, -3, \dots$, the distributions of the bisection type x_+^λ and x_-^λ in Eq. (43) are defined as (Gel'fand and Shilov, 1964)

$$x_+^\lambda = \begin{cases} |\bar{x}|^\lambda, & \bar{x} > 0 \\ 0, & \bar{x} < 0 \end{cases} \quad \text{and} \quad x_-^\lambda = \begin{cases} 0, & \bar{x} > 0 \\ |\bar{x}|^\lambda, & \bar{x} < 0 \end{cases}. \tag{45}$$

The integral in Eq. (43) is evaluated using Fisher's theorem for products of distributions of the bisection type (Fisher, 1971). More specifically, we employ the relation $(x_+)^{-1-\lambda} (x_-)^\lambda = -\pi \delta(x) [2 \sin(\pi\lambda)]^{-1}$, where $\lambda \neq -1, -2, -3, \dots$ and $\delta(x)$ is the Dirac delta distribution, as well as the fundamental property of the Dirac delta distribution, i.e.,

$$\int_{-\varepsilon}^{\varepsilon} \delta(x) dx = 1.$$

A strictly analogous procedure is followed for the evaluation of the J -integral at the left crack-tip. In this case, we obtain the following result

$$J_\ell = -\frac{\mu\pi}{2} a \left[\Lambda_1^{(\ell)} + \left(\frac{\ell}{a} \right)^2 \Lambda_2^{(\ell)} \right], \tag{46}$$

where

$$\Lambda_1^{(\ell)} = \frac{(3-2\nu)}{4(1-\nu)} \left(\sum_{n=1}^N (-1)^n b_n \right)^2, \quad \Lambda_2^{(\ell)} = \left(\sum_{n=1}^N (-1)^n c_n \right)^2. \quad (47)$$

The corresponding values for the J -integral in classical elasticity may be obtained in closed form by utilizing a similar contour as the one used earlier and the elastic fields of the problem. Indeed, following the same procedure as described above, we obtain the following forms for the J -integral at the right and left crack-tips

$$\begin{aligned} J_r^{clas.} &= \frac{\mu b_y^2 \left[1 - \left(\frac{d+a}{d-a} \right)^{1/2} \right] \left[d-a - (d^2-a^2)^{1/2} \right]}{8\pi a(1-\nu)(d-a)}, \\ J_\ell^{clas.} &= - \frac{\mu b_y^2 \left[1 - \left(\frac{d+a}{d-a} \right)^{1/2} \right] \left[d-a - (d^2-a^2)^{1/2} \right]}{8\pi a(1-\nu)(d+a)}. \end{aligned} \quad (48)$$

To the best of our knowledge, these expressions were not available in the literature and these are given here for the first time.

Besides evaluating the energy release rate at the crack-tips, it is interesting to calculate the driving force exerted on the discrete climb dislocation due to its interaction with the finite-length crack. The well-known Peach-Koehler force may be calculated based on its definition using the expression for the normal stress σ_{yy} (Eq. (51)), excluding the contribution of the discrete climb dislocation $\sigma_{yy}^{(b_y)}$ (Dundurs and Markenscoff, 1989). Alternatively, considering a contour that surrounds both the crack and the discrete dislocation (Fig. 4) and using the connection between Peach-Koehler force and J -integral around a dislocation (Eshelby, 1951; Ni and Markenscoff, 2008), we may write the expression

$$F_x^{sd} = -(J_r + J_\ell), \quad (49)$$

where F_x^{sd} (or equivalently J_d) is the Peach-Koehler force in the x -direction for the discrete climb dislocation (Fig. 4). In the next Section, the Peach-Koehler force will be calculated based on its definition and verified using Eq. (49). The latter expression is another way to assess the convergence of the numerical solution. The relevant value for the Peach-Koehler force in classical elasticity is given as (Zhang and Li, 1991)

$$F_x^{sd, clas.} = -\frac{\mu b_y^2}{2\pi(1-\nu)} \frac{d - (d^2 - a^2)^{1/2}}{d^2 - a^2}. \quad (50)$$

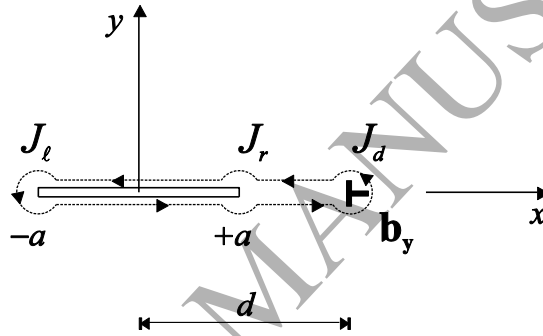


Fig. 4: Contour for the calculation of Peach-Koehler force around the discrete climb dislocation.

8. Results and discussion

In this Section, we present representative results with a view toward highlighting the deviations from the classical elasticity theory when couple-stresses are introduced. In Fig. 5a the dependence of the normal crack-face displacement (Eq. (24)) upon the ratio a/ℓ is displayed for a climb dislocation lying at a distance $d/a = 2.5$ for a couple-stress material with Poisson's ratio $\nu = 0.3$. It is observed that as the crack length becomes comparable to the characteristic length ℓ , the material exhibits a more stiff behaviour, i.e. the crack-face displacements become smaller in magnitude compared to the respective ones in classical elasticity (rigidity effect). Further, it is

noted that the classical elasticity solution (dashed line) serves as an upper bound for couple-stress elasticity. In Fig. 5b the influence of the dislocation distance to the crack-face displacement is examined. The material properties are $a/\ell = 10$ and $\nu = 0.3$. The resulting displacements vary significantly both in shape and magnitude. It is recalled that in the limit case $d/a = 1.0$ (dislocated crack problem), the loading in the left hand side of Eq. (35) and (36) vanishes and the contribution of the dislocation is introduced through the complementary conditions (27). In that case, the crack remains open at one end. It is observed that the shape of the ‘dislocated crack’ differs significantly from the classical solution (Tada et al, 2000) when couple-stresses are considered.

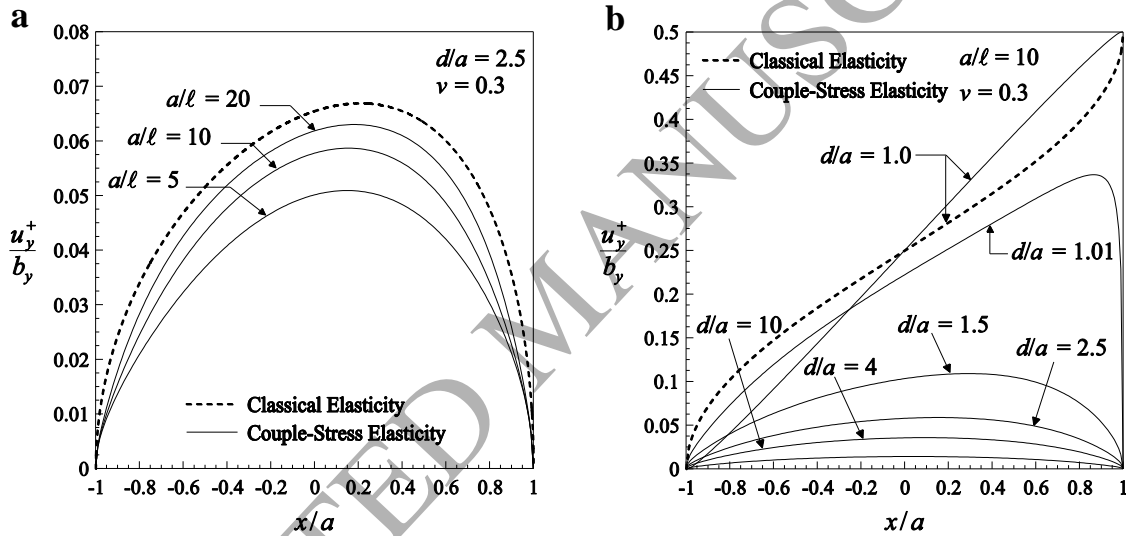


Fig. 5: **a)** Normalized upper-half crack face displacement profile for various ratios a/ℓ due to the interaction with a climb dislocation lying at $d/a = 2.5$. **b)** Normalized upper-half crack face displacement profile for various dislocation positions in a material with $a/\ell = 10$. The Poisson's ratio is $\nu = 0.3$ in all cases.

Accordingly, using Eq. (25), we calculate the upper-half crack rotation for the same cases. In Fig. 6a the variation of the upper crack-face rotation for several values of the ratio a/ℓ is depicted. It is observed that the produced fields are *bounded* contrary to the prediction of classical elasticity where the rotation exhibits a square-root singularity at the crack-tips. Note that as $\ell \rightarrow 0$, the rotation becomes pointwise convergent to the respective unbounded rotation in classical elasticity, revealing, thus, a boundary layer effect in the solution of couple-stress

theory. In Fig. 6b the change in the rotation profile for different distances of the discrete dislocation is presented. It is noted that as the dislocation approaches the crack, the rotation of the right crack-tip increases significantly. In the special case $d/a \rightarrow 1$ the rotation is positive throughout the crack length since the displacement field is increasing monotonically.

Next, we examine the behavior of the normal stress σ_{yy} and couple-stress m_{yz} ahead of the crack-tip. Employing Eqs (22) and (23), we derive the expressions

$$\begin{aligned} \sigma_{yy}(|x| > a, 0) = & \sigma_{yy}^{(b_y)}(x-d, 0) + \frac{\mu(3-2\nu)}{2\pi(1-\nu)} \int_{-a}^a \frac{B_l(t)}{x-t} dt + \frac{\mu}{\pi a} \int_{-a}^a W(t) \ln \frac{|x-t|}{\ell} dt \\ & + \frac{2\mu}{\pi a} \int_{-a}^a B_l(t) R_1(x-t) dt - \frac{\mu}{\pi a} \int_{-a}^a W(t) R_2(x-t) dt \end{aligned} \quad (51)$$

$$\begin{aligned} m_{yz}(|x| > a, 0) = & m_{yz}^{(b_y)}(x-d, 0) - \frac{2\mu\ell^2}{\pi a} \int_{-a}^a \frac{W(t)}{x-t} dt + \frac{\mu}{\pi} \int_{-a}^a B_l(t) \ln \frac{|x-t|}{\ell} dt \\ & - \frac{\mu}{\pi} \int_{-a}^a B_l(t) R_2(x-t) dt + \frac{\mu\ell}{2\pi a} \int_{-a}^a W(t) R_3(x-t) dt \end{aligned} \quad (52)$$

The integrals in Eqs. (51) and (52) are not singular for $|x| > a$ and are evaluated in closed form using Eqs (B3) and (B4) in Appendix B. Moreover, in view of Eqs (39) and (40), it is readily inferred that both the normal stress σ_{yy} and the couple-stress m_{yz} exhibit a square-root singularity ahead of the crack-tips ($x \rightarrow \pm a$). This conclusion is in agreement with the asymptotic results of Sternberg and Muki (1967) and Huang et al. (1997).

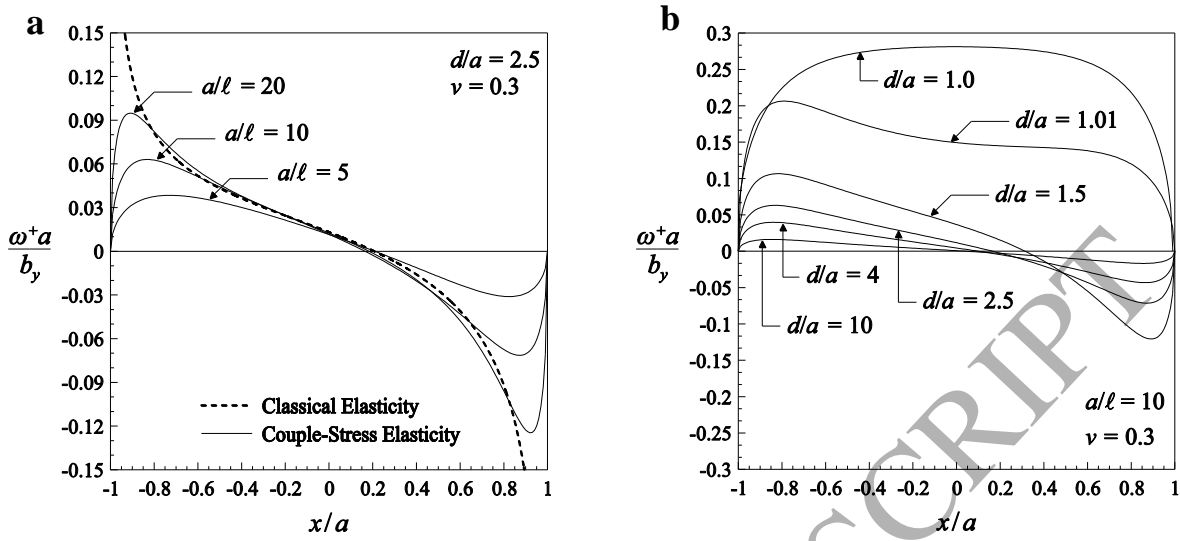


Fig. 6: **a)** Normalized upper-half crack rotation profile for various ratios a/ℓ due to the interaction with a climb dislocation lying at $d/a = 2.5$. **b)** Normalized upper-half crack rotation profile for various dislocation positions in a material with $a/\ell = 10$. The Poisson's ratio is $\nu = 0.3$ in all cases.

In Fig. 7a, the distribution of the normal stress σ_{yy} (Eq. (51)) due to the interaction with a discrete climb dislocation lying at a distance $d/a = 2.5$ is given, in a medium with $a/\ell = 10$ and Poisson's ratio $\nu = 0.3$. For convenience, a new variable $\bar{x} = x - a$ is introduced that measures the distance ahead of the right crack-tip. We notice that the couple-stress effects are dominant within a zone of length 3ℓ near the crack-tip and 5ℓ around the dislocation core. Outside this zone the field gradually approaches the distribution given by classical elasticity. The solution depends upon the ratio a/ℓ and the Poisson's ratio, as shown in Eq. (51). The Cauchy type singularity for the σ_{yy} stress induced by the dislocation is retained also in couple-stress theory. Qualitatively similar distributions for the stress field are observed for all distances of the discrete edge dislocation except for the special case $d/a \rightarrow 1$. As seen in Fig. 7a, the normal stress in this case is negative for all $\bar{x} > 0$ since the dislocation is now situated at the right crack-tip. The distribution of the couple-stress m_{yz} (52) is plotted in Fig. 7b. Again, the couple-stress effects are significant in a zone of length 3ℓ ahead of the crack-tip and 10ℓ around the dislocation core. At

the point of the dislocation tip ($\bar{x}/\ell = 15$), the couple-stress becomes logarithmically unbounded as is predicted by Eqs (19)-(21).

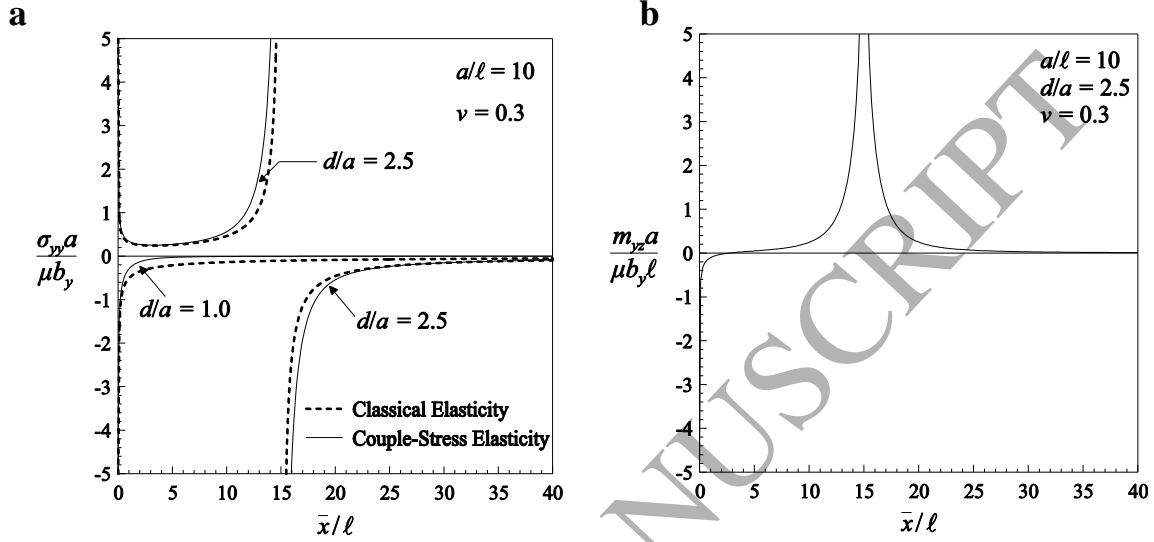


Fig. 7: Variation of **a)** the normal stress σ_{yy} and **b)** the couple-stress m_{yz} ahead of the right crack-tip due to the interaction with a climb dislocation lying at $d/a = 2.5$ in a medium with $a/\ell = 10$ and Poisson's ratio $\nu = 0.3$.

Next, we examine the variation of the stress intensity factor (SIF) in both crack-tips in couple-stress theory. For the right crack-tip, the SIF is defined as $K_I = \lim_{x \rightarrow a^+} [2\pi(x-a)]^{1/2} \sigma_{yy}(x, 0)$, where the asymptotic behavior of the normal stress $\sigma_{yy}(x, 0)$ is provided in Eq. (39)₁. The SIF at the left crack-tip is determined in a similar manner. In Fig. 8a, the variation of the ratio $K_I/K_I^{clas.}$ on both crack-tips with respect to the ratio ℓ/a and the Poisson's ratio ν is depicted, for a climb dislocation lying at $d/a = 2.5$. It is observed that the ratio of the SIFs depends significantly on the Poisson's ratio and that there is a general increase when couple-stress effects are considered for any microstructural ratio ℓ/a (stress aggravation). The response is significantly different in the two crack-tips due to the asymmetric loading imposed. The right crack-tip curves (continuous lines) monotonically increase as the ratio ℓ/a increases, while the left crack-tip response (dashed lines) shows an initial decreasing branch and

then increases as the couple-stress effects become more prominent. It should be noted that in the case $\ell/a = 0$ (no couple-stress effects considered), the above ratio should evidently approach unity. On the contrary, the SIFs ratio exhibits a *finite* jump discontinuity at the limit $\ell/a = 0$. This behavior has been reported in the past in many crack problems in the framework of couple-stress theory. Sternberg and Muki (1967) attributed this behavior to the severe boundary layer effects arising in couple-stress elasticity in singular stress-concentration problems. It should be finally noted that as $\ell/a \rightarrow \infty$, the ratio $K_I/K_I^{clas.}$ approaches asymptotically the value $(3-2\nu)$.

Table 1: Convergence of the SIFs ratio $K_{I,r}/K_{I,r}^{clas.}$ at the right crack-tip for increasing collocation points N .

The climb dislocation lies at a distance $d/a = 2.0$ in a couple-stress material with Poisson's ratio $\nu = 0$.

N	$\ell/a = 1.0$	$\ell/a = 0.8$	$\ell/a = 0.5$	$\ell/a = 0.2$	$\ell/a = 0.1$	$\ell/a = 0.05$	$\ell/a = 0.01$	$\ell/a = 0.005$
10	2.61055	2.47282	2.11815	1.52564	1.35979	1.33328	1.88755	2.31070
20	2.61055	2.47282	2.11816	1.52565	1.35930	1.31383	1.33701	1.51537
30			2.11816	1.52565	1.35930	1.31382	1.30031	1.32368
40						1.31382	1.29958	1.30113
50							1.29945	1.29925
60							1.29945	1.29924
70								1.29924

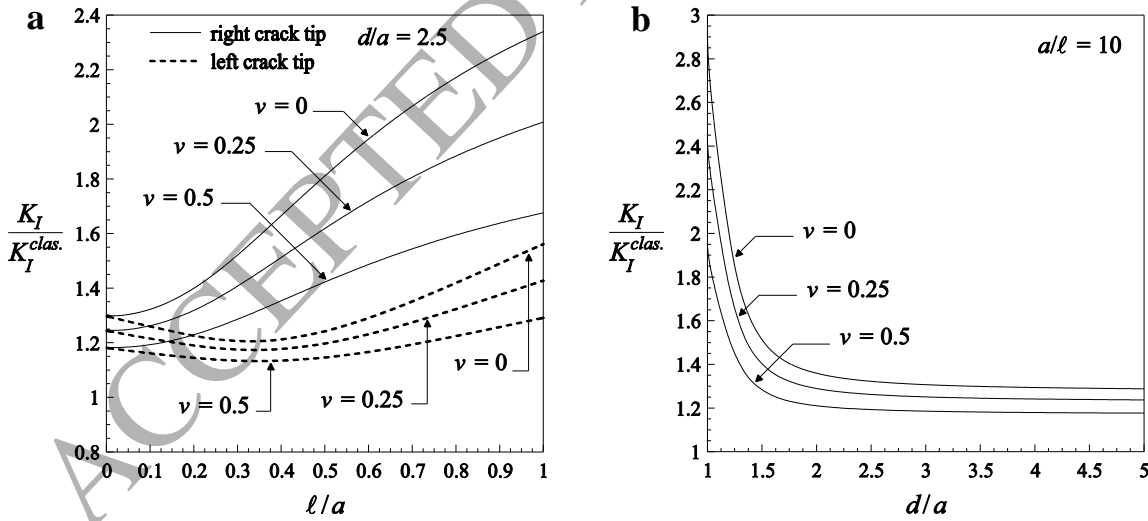


Fig. 8: a) Variation of the ratio of SIFs $K_I/K_I^{clas.}$ in couple-stress theory and in classical elasticity with ℓ/a for a climb dislocation lying at $d/a = 2.5$. b) Variation of $K_I/K_I^{clas.}$ in the right crack-tip with the dislocation distance d/a in a material with $a/\ell = 10$.

In Fig. 8b, the variation of the ratio $K_I/K_I^{clas.}$ ahead of the right crack-tip is plotted for various values of the dislocation distance d/a and the Poisson's ratio ν in a medium with $a/\ell = 10$. The ratio diminishes monotonically as the dislocation is placed farther from the crack-tip and quickly reaches a constant value. This value coincides with the corresponding value of the ratio in the problem of a finite-length crack under constant remote loading (mode I), for the same ratio a/ℓ . Indeed, Gourgiotis and Georgiadis (2008) reported a ratio of 1.28 for $\ell/a = 0.1$ and $\nu = 0$ while for $\nu = 0.25$ and $\nu = 0.5$ the values are 1.23 and 1.17, respectively. A similar response is observed at the left crack-tip.

Based on the analysis presented in Section 6, the ERR (crack driving force) is evaluated next and its dependence upon the microstructural ratio ℓ/a , the Poisson's ratio ν , and the distance of the dislocation from the crack-tip is investigated. In particular, in Fig. 9a the variation of the ratio $J/J^{clas.}$ on both crack-tips with respect to ℓ/a and the Poisson's ratio ν is illustrated, for a climb dislocation lying at $d/a = 2.5$. Contrary to the SIF behavior, we observe that as $\ell/a \rightarrow 0$ the J -integral in couple-stress theory tends to the corresponding result of classical elasticity. In particular, as $\ell/a \rightarrow 0$ the second term in the J -integral (38), regarding the couple-stress contribution, becomes vanishingly small. This can be easily checked by inspection of the asymptotic relations (40) and (42). On the other hand, regarding the first (standard) term in the J -integral (38), we remark that although the SIF increases as compared to its classical value (stress aggravation effect), the crack face displacement u_y decreases significantly (see Fig. 5) compensating for the increase in the SIF. Hence, the as $\ell/a \rightarrow 0$ this term converges to the classical elasticity result. This behavior of the J -integral has been reported also in other crack problems in couple-stress theory (see e.g. Atkinson and Leppington, 1977; Gourgiotis and Georgiadis, 2008; Gourgiotis et al., 2012). It should be noted that in all curves, as ℓ/a increases, an initial decreasing response of the ratio is observed ($J < J^{clas.}$) until a minimum value is reached for $0.2 \leq \ell/a \leq 0.25$ (this range varies depending on the Poisson's ratio and the dislocation distance d/a) and then the ratio increases monotonically ($J > J^{clas.}$). Therefore, for small values of the ratio ℓ/a the ERR decreases as compared to the classical value showing a

strengthening effect when couple-stresses are taken into account (Gourgiotis and Georgiadis, 2008; Gourgiotis and Piccolroaz, 2014). However, as ℓ/a increases further (the couple-stress effects become more pronounced) the ratio $J/J^{clas.}$ increases above unity revealing, thus, an interesting *weakening* effect. The term weakening is justified from the fact that the crack driving force is increased as compared to the classical value when the couple-stress effects are dominant. In fact, assuming that J_c is the experimentally observed (under specific environmental conditions) critical value of the ERR at which crack advancement occurs, it may happen that couple-stress elasticity predicts that $J > J_c$, while $J^{clas.} < J_c$. It is worth noting that a similar behavior was observed in the context of couple-stress elasticity in the cases of: (i) a crack loaded by concentrated shear force at the crack faces (Gourgiotis et al. 2012) and (ii) in a mode-III steady state propagating crack loaded by a distribution of antiplane shear tractions along the crack faces (Morini et al. 2014). Finally, it is remarked that as $\ell/a \rightarrow \infty$ the ratio tends asymptotically to the value $(3 - 2\nu)$.

In Fig. 9b, the variation of the ratio $J/J^{clas.}$ at the right crack-tip is presented with respect to the dislocation distance d/a and the Poisson's ratio ν for a couple-stress medium with $a/\ell = 10$. The behavior is similar to the one exhibited by the SIFs ratio (Fig. 8b), monotonically decreasing until a constant value is reached. Again, this limiting value can be related to the corresponding value of the ratio $J/J^{clas.}$ in the mode-I crack problem. In particular, as it was shown by Gourgiotis and Georgiadis (2008), the ratio reaches a value of 0.86 for a couple-stress material with $\ell/a = 0.1$ and $\nu = 0$, while for $\nu = 0.25$ and $\nu = 0.5$ the ratio becomes 0.88 and 0.92, respectively. An analogous response is reported for the left crack-tip.

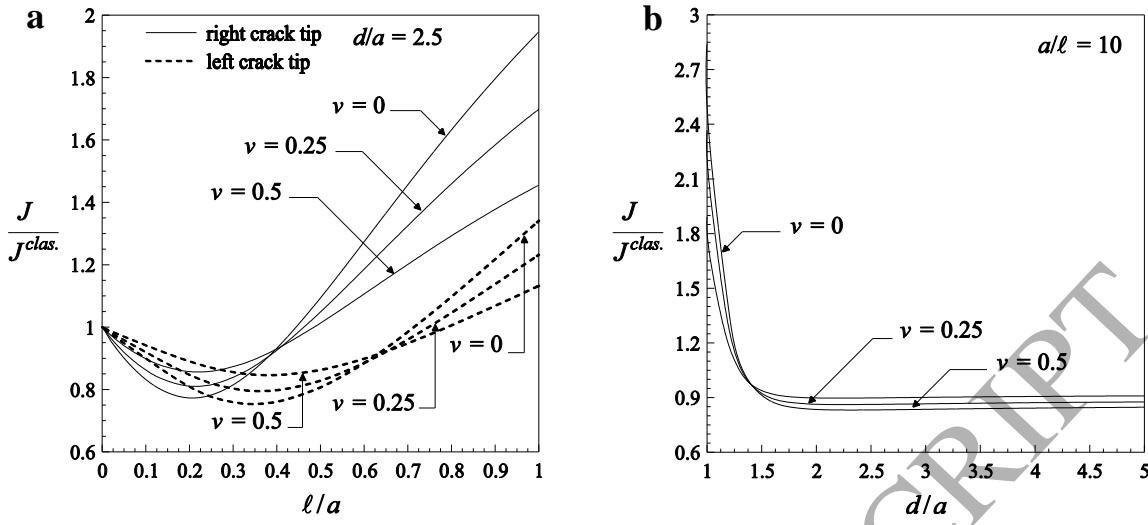


Fig. 9: **a)** Variation of the ratio of J -integrals ($J/J^{clas.}$) in couple-stress theory and in classical elasticity **a)** with respect to ℓ/a for a climb dislocation lying at $d/a = 2.5$. **b)** with respect to the dislocation distance d/a in a material with $a/\ell = 10$.

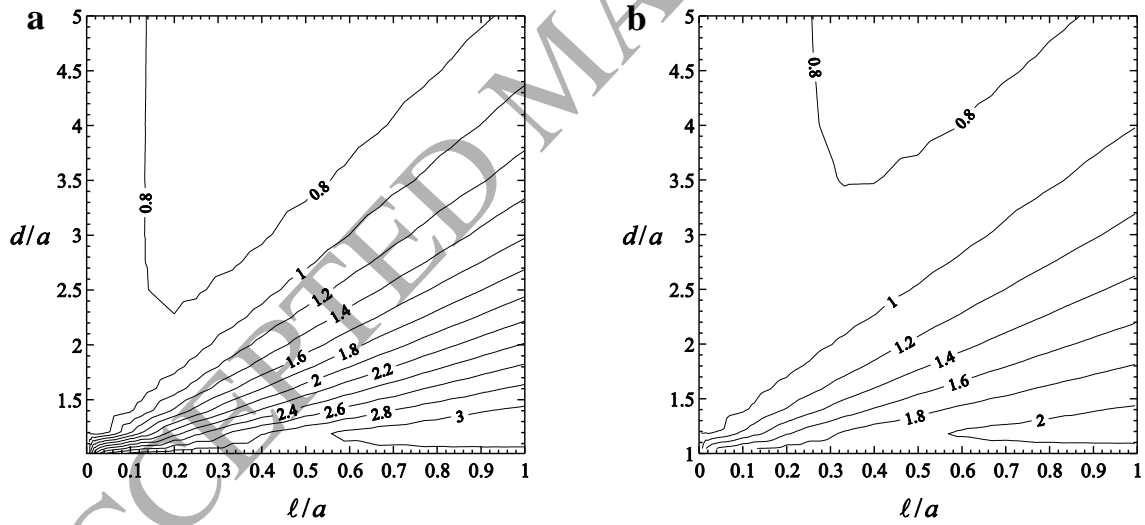


Fig. 10: Level sets of the ratio $J/J^{clas.}$ with respect to ℓ/a and d/a for Poisson's ratios **a)** $\nu = 0$ and **b)** $\nu = 0.5$.

In order to further explore the phenomenon of decrease or increase of the ERR in couple-stress theory as presented in Fig. 9a, we attempt a parametric analysis of the problem for various

values of the ratios ℓ/a , d/a , and Poisson's ratio. In Fig. 10 the effect of ℓ/a and d/a upon the ratio $J/J^{clas.}$ at the right crack-tip is depicted, for Poisson's ratios $\nu = 0$ (Fig. 10a) and $\nu = 0.5$ (Fig. 10b). The contour $J/J^{clas.} = 1$ sets the limit between increase and decrease of the ERR (or the crack driving force) in couple-stress elasticity as compared to the respective one in the classical theory. Therefore, there is a distinct region defined by the contour $J/J^{clas.} = 1$ as $d/a \rightarrow 1$, where the energy release rate or the crack driving force increases in couple-stress theory. The area of this region diminishes as the Poisson's ratio increases.

In light of the previous results regarding the behavior of the J -integral, we anticipate also the Peach-Koehler force exerted on the dislocation to depend strongly upon the characteristic length ℓ , the distance d , and the Poisson's ratio ν . In Fig. 11, the dependence of the ratio $F_x^{sd}/F_x^{sd,clas.}$ on the ratios ℓ/a and d/a is presented in an isocontour plot for Poisson's ratios $\nu = 0$ (Fig. 11a) and $\nu = 0.5$ (Fig. 11b). In accordance to the results obtained for the J -integral, a region on the right of the contour $F_x^{sd}/F_x^{sd,clas.} = 1$ is formed where the value of the Peach-Koehler force is higher in couple-stress theory, predicting a weakening effect for the material under consideration. The area of this region is larger compared to the relevant region for the J -integral (Fig. 10) and reduces as the Poisson's ratio increases.

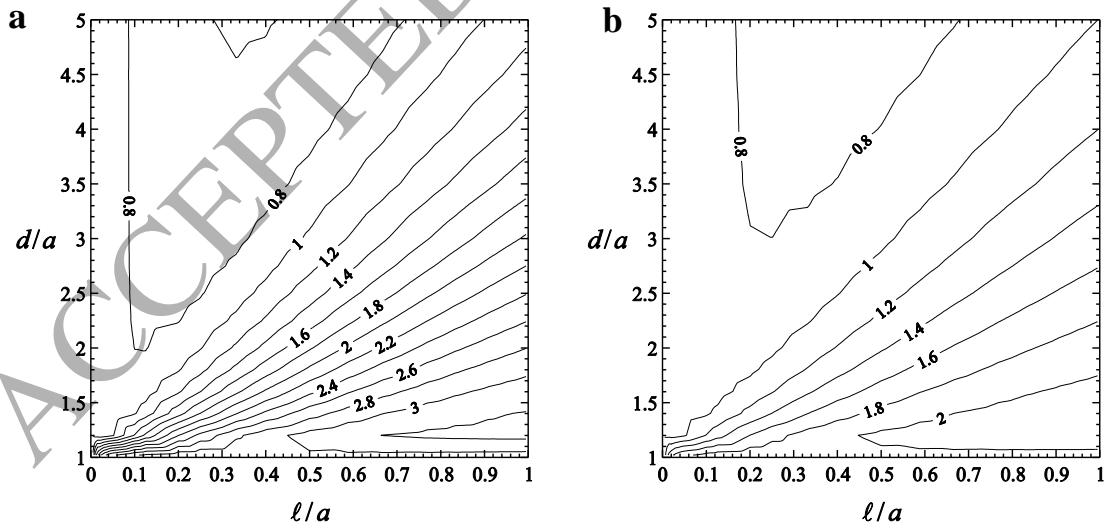


Fig. 11: Variation of the ratio $F_x^{sd}/F_x^{sd,clas.}$ with respect to ℓ/a and d/a for Poisson's ratios **a)** $\nu = 0$ and **b)** $\nu = 0.5$.

9. Concluding remarks

In the present study, the interaction of a discrete climb dislocation with a finite-length crack in the framework of couple-stress elasticity was investigated. The crack problem was solved using the distributed dislocation technique. In order to satisfy the boundary conditions that arise in couple-stress elasticity, both translational and rotational defects need to be distributed along the crack faces. The necessary rotational defect which was previously coined as ‘constrained’ wedge disclination in fact corresponds to crystal twinning. Following the standard distributed dislocation approach, the interaction problem was modeled by a system of coupled singular integral equations with Cauchy and logarithmic kernels which was accordingly solved numerically using an appropriate collocation technique.

Several interesting and novel results were revealed comparing the present solution to the classical one. Looking at the kinematics, a rigidity effect was observed, i.e. the crack-face displacements become smaller in magnitude than their counterparts in classical elasticity when the crack length is comparable with the characteristic material length. Accordingly, the produced rotation field becomes bounded contrary to the prediction of classical elasticity. Regarding the stress and couple-stress fields, it was shown that the couple-stress effects are dominant within a small zone adjacent to the crack-tip and around the dislocation core. Both fields remain unbounded around the defects tips, while the stress level within a small zone adjacent to the tip is significantly higher than the classical one. The behavior of the driving (configurational) forces at the crack-tips and at the climb dislocation was thoroughly examined. It was shown that the ERR at the crack-tips and the Peach-Koehler force at the dislocation may either become lower than the ones predicted by the classical elasticity revealing, thus, a strengthening effect, or higher providing a weakening effect estimation. This alternating behavior depends upon the distance between the crack-tip and the dislocation core as well as the magnitude of the characteristic material length with respect to the length of the crack.

Acknowledgments

The authors are thankful to Prof. X. Markenscoff (University of California, San Diego) for fruitful discussions.

Appendix A

The expressions for the displacement, stress, and couple-stress fields due to a single climb dislocation with Burgers vector $\mathbf{b} = (0, b_y, 0)$ and a constrained wedge disclination with Frank vector $\mathbf{\Omega} = (0, 0, \Omega)$ lying in an infinite couple-stress isotropic medium are derived here in closed form. The boundary value problems for the two defects, as described by Eqs. (16) and (17), are attacked employing a Fourier transform analysis. The direct Fourier transform and its inverse are defined as

$$f^*(\xi, y) = \frac{1}{(2\pi)^{1/2}} \int_{-\infty}^{\infty} f(x, y) e^{ix\xi} dx, \quad f(x, y) = \frac{1}{(2\pi)^{1/2}} \int_{-\infty}^{\infty} f^*(\xi, y) e^{-ix\xi} d\xi, \quad (\text{A1})$$

where $i \equiv (-1)^{1/2}$. Transforming the field Eqs. (11) and (12), we obtain a system of ordinary differential equations in terms of the transformed displacements (u_x^*, u_y^*) which has the following bounded solution as $y \rightarrow +\infty$

$$u_x^*(\xi, y) = A_1(\xi) e^{-|\xi|y} + A_2(\xi) y e^{-|\xi|y} + A_3(\xi) e^{-y\alpha}, \quad (\text{A2})$$

$$u_y^*(\xi, y) = -i \operatorname{sgn}(\xi) A_1(\xi) + \left[\frac{(3-4\nu)}{\xi} - i \operatorname{sgn}(\xi) y \right] A_2(\xi) e^{-|\xi|y} - i \frac{\xi}{\alpha} A_3(\xi) e^{-\frac{y\alpha}{\ell}}, \quad (\text{A3})$$

where $\alpha \equiv \alpha(\xi) = (1 + \ell^2 \xi^2)^{1/2}$, $\operatorname{sgn}(\)$ denotes the signum function, and $A_q(\xi)$ are unknown functions that will be determined through the enforcement of the boundary conditions of each problem. Applying the Fourier transform to the boundary conditions (16) and (17), we derive

$$u_y^*(\xi, 0^+) = -b_y (\pi/2)^{1/2} \delta_+(\xi), \quad \omega^*(\xi, 0^+) = 0, \quad \sigma_{yx}^*(\xi, 0^+) = 0, \quad (\text{A4})$$

$$u_x^*(\xi, 0^+) = 0, \quad \omega^*(\xi, 0^+) = \Omega (\pi/2)^{1/2} \delta_+(\xi), \quad \sigma_{yx}^*(\xi, 0^+) = 0, \quad (\text{A5})$$

where $\delta_+(\xi) = [\delta(\xi)/2] + [i/2\pi\xi]$ is the Heisenberg delta function (see e.g. Roos, 1969) and $\delta(\xi)$ is the Dirac delta distribution. It should be mentioned that the contribution of the Dirac delta distribution corresponds to a rigid body displacement in the dislocation problem and a rigid body rotation in the disclination problem.

Further, combining equations (A2)-(A3). and using, accordingly, the inverse Fourier transform and results from the theory of distributions (Roos, 1969; Gourgiotis and Georgiadis, 2008), the final expressions for the displacements assume the following form

$$u_x(x, y) = \frac{b_y(1-2\nu)}{4\pi(1-\nu)} \ln r + \frac{b_y(y^2-x^2)}{8\pi(1-\nu)r^2} - \frac{b_y(y^2-x^2)}{2\pi r^2} \left[\frac{2\ell^2}{r^2} - K_2\left(\frac{r}{\ell}\right) \right] + \frac{b_y}{2\pi} K_0\left(\frac{r}{\ell}\right) - \frac{\Omega \ell^2 x}{r^2} + \frac{\Omega \ell}{\pi} I_{11} + \frac{\Omega y}{4}, \quad (A6)$$

$$u_y(x, y) = \frac{b_y}{2\pi} \tan^{-1}\left(\frac{y}{x}\right) - \frac{b_y xy}{4\pi(1-\nu)r^2} + \frac{b_y xy}{\pi r^2} \left[\frac{2\ell^2}{r^2} - K_2\left(\frac{r}{\ell}\right) \right] - \frac{\Omega y}{2\pi} \left[\frac{2\ell^2}{r^2} - K_2\left(\frac{r}{\ell}\right) \right] - \frac{\Omega y}{2\pi} K_2\left(\frac{r}{\ell}\right) - \frac{\Omega x}{4}, \quad (A7)$$

and, accordingly, the rotation ω becomes

$$\omega(x, y) = -\frac{b_y y}{4\pi \ell^2} \left[\frac{2\ell^2}{r^2} - K_2\left(\frac{r}{\ell}\right) \right] - \frac{b_y y}{4\pi \ell^2} K_0\left(\frac{r}{\ell}\right) + \frac{\Omega}{2\pi} I_{10} - \frac{\Omega}{4}, \quad (A8)$$

where $I_{10} \equiv I_{10}(x, y) = \int_0^\infty \xi^{-1} e^{-\frac{y\xi}{\ell}} \sin(\xi x) d\xi$, and $I_{11} = -\ell \partial_y (I_{10})$. It should be noted that a rigid body displacement ($b_y/4$) and rotation ($-\Omega/4$) have been added in Eqs. (A7) and (A8), so that the normal displacement u_y and the rotation ω are null at the plane ($y=0^+$, $x>0$).

The full field solution for the stresses and couple-stresses resulting from the superposition of the two defects is obtained then using Eqs. (A6)-(A8) and the constitutive equations (5), (6), in conjunction with Eqs. (7)-(10)[#]

$$\sigma_{xx} = \frac{\mu b_y x}{2\pi(1-\nu)} \frac{(x^2 - y^2)}{r^4} + \frac{2\mu b_y x}{\pi} \frac{(3y^2 - x^2)}{r^4} \left[\frac{2\ell^2}{r^2} - K_2\left(\frac{r}{\ell}\right) \right] - \frac{\mu b_y}{\pi \ell^2} \frac{xy^2}{r^2} \left[K_2\left(\frac{r}{\ell}\right) - K_0\left(\frac{r}{\ell}\right) \right] + \frac{\mu \Omega (x^2 - y^2)}{\pi r^2} \left[\frac{2\ell^2}{r^2} - K_2\left(\frac{r}{\ell}\right) \right] + \frac{\mu \Omega}{\pi} K_0\left(\frac{r}{\ell}\right), \quad (\text{A9})$$

$$\sigma_{yy} = \frac{\mu b_y x}{2\pi(1-\nu)} \frac{(3y^2 + x^2)}{r^4} - \frac{2\mu b_y x}{\pi} \frac{(3y^2 - x^2)}{r^4} \left[\frac{2\ell^2}{r^2} - K_2\left(\frac{r}{\ell}\right) \right] + \frac{\mu b_y}{\pi \ell^2} \frac{xy^2}{r^2} \left[K_2\left(\frac{r}{\ell}\right) - K_0\left(\frac{r}{\ell}\right) \right] - \frac{\mu \Omega (x^2 - y^2)}{\pi r^2} \left[\frac{2\ell^2}{r^2} - K_2\left(\frac{r}{\ell}\right) \right] - \frac{\mu \Omega}{\pi} K_0\left(\frac{r}{\ell}\right), \quad (\text{A10})$$

$$\sigma_{yx} = \frac{\mu b_y}{2\pi(1-\nu)} \frac{y(x^2 - y^2)}{r^4} - \frac{2\mu b_y y}{\pi} \frac{(3x^2 - y^2)}{r^4} \left[\frac{2\ell^2}{r^2} - K_2\left(\frac{r}{\ell}\right) \right] + \frac{\mu b_y}{\pi \ell^2} \frac{yx^2}{r^2} \left[K_2\left(\frac{r}{\ell}\right) - K_0\left(\frac{r}{\ell}\right) \right] + \frac{2\mu \Omega xy}{\pi r^2} \left[\frac{2\ell^2}{r^2} - K_2\left(\frac{r}{\ell}\right) \right], \quad (\text{A11})$$

$$\sigma_{xy} = \sigma_{yx} - 4\mu \ell^2 \nabla^2 \omega, \quad (\text{A12})$$

$$m_{xz} = -\frac{2\mu b_y}{\pi} \frac{xy}{r^2} \left[K_2\left(\frac{r}{\ell}\right) - \frac{2\ell^2}{r^2} \right] + \frac{\mu \Omega}{\pi} y \left[K_2\left(\frac{r}{\ell}\right) - K_0\left(\frac{r}{\ell}\right) \right], \quad (\text{A13})$$

$$m_{yz} = \frac{\mu b_y}{\pi} \frac{(x^2 - y^2)}{r^2} \left[K_2\left(\frac{r}{\ell}\right) - \frac{2\ell^2}{r^2} \right] - \frac{\mu b_y}{\pi} K_0\left(\frac{r}{\ell}\right) - \frac{2\mu \ell \Omega}{\pi} I_{11}. \quad (\text{A14})$$

[#] Note that in Gourgiotis and Georgiadis (2008) the expressions for σ_{xx} and σ_{yy} (see Eqs. (A8) and (A9) in that paper) contained a misprint that does not, however, affect their final results in any way.

It is interesting to note that for $y = 0$, the integral I_{11} is evaluated analytically as

$$I_{11}(x, 0) = -\frac{1}{4} \operatorname{sgn}(x) G_{1,3}^{2,1} \left(\frac{x^2}{4\ell^2} \middle| \begin{matrix} 1 \\ -1/2, 1/2, 0 \end{matrix} \right), \quad (\text{A15})$$

where $G_{c,d}^{a,b}(\cdot)$ is the MeijerG function (see e.g. Erdélyi et al., 1953; Abramowitz and Stegun, 1964).

In view of the above, the influence functions of the problem are derived in *closed* form and provided in Eqs (19) and (20). Finally, it is remarked that once the dislocation density $B_l(t)$ and the disclination density $W(t)$ (Eqs. (24) and (25)) are evaluated, the stresses and couple-stresses at any point of the cracked body can be obtained utilizing Eqs. (A9)-(A14).

Appendix B

In this Appendix, we provide the closed-form expressions for the singular (Cauchy) and weakly singular (logarithmic) integrals involving Chebyshev polynomials that were utilized in Section 5.

For $|x| < 1$, these integrals are computed as (see e.g. Chrysakis and Tsamasphyros, 1992; Chan et al. 2003)

$$\int_{-1}^1 \frac{T_n(t)(1-t^2)^{-1/2}}{x-t} dt = \begin{cases} 0, & n = 0 \\ -\pi U_{n-1}(x), & n \geq 1 \end{cases}, \quad (\text{B1})$$

$$\int_{-1}^1 T_n(t)(1-t^2)^{-1/2} \ln(|x-t|) dt = \begin{cases} -\pi \ln 2, & n = 0 \\ -\frac{\pi}{n} T_n(x), & n \geq 1 \end{cases}, \quad (\text{B2})$$

where $T_n(t)$ are the Chebyshev polynomials of the first kind.

For $|x| > 1$, the above integrals are no longer singular and are evaluated according to the following expressions

$$\int_{-1}^1 \frac{T_n(t)(1-t^2)^{-1/2}}{x-t} dt = \pi \operatorname{sgn}(x) \frac{\left[x - \operatorname{sgn}(x)(x^2-1)^{1/2} \right]^n}{(x^2-1)^{1/2}}, \quad n \geq 0, \quad (\text{B3})$$

$$\int_{-1}^1 T_n(t)(1-t^2)^{-1/2} \ln(|x-t|) dt = \begin{cases} \pi \operatorname{sgn}(x) \ln \left[x + (x^2-1)^{1/2} \right] & n=0, \\ -\pi \ln 2, & \\ -\frac{\pi}{n} \left[x - \operatorname{sgn}(x)(x^2-1)^{1/2} \right]^n, & n \geq 1. \end{cases} \quad (\text{B4})$$

References

- Abramowitz, M., Stegun, I.A., 1964. Handbook of mathematical functions. National Bureau of Standards, Applied Mathematics Series 55.
- Anthony, K.-H., 1970. Die theorie der disklinationen. Arch. Ration. Mech. Anal. 39, 43-88.
- Atkinson, C., Leppington, F.G., 1974. Some calculations of the energy-release rate G for cracks in micropolar and couple-stress elastic media. Int. J. Fract. 10, 599-602.
- Atkinson, C., Leppington, F.G., 1977. The effect of couple stresses on the tip of a crack. Int. J. Solids Struct. 13, 1103-1122.
- Barenblatt, G.I., 1962. The mathematical theory of equilibrium cracks in brittle fracture, Advances in Applied Mechanics. Elsevier, pp. 55-129.
- Bigoni, D., Gourgiotis, P.A., 2016. Folding and faulting of an elastic continuum. Proc. R. Soc. Lond. A, 472(2187): 20160018.
- Burridge, R., 1976. An influence function for the intensity factor in tensile fracture. Int. J. Eng. Sci. 14, 725-734.
- Chan, Y.-S., Fannjiang, A.C., Paulino, G.H., 2003. Integral equations with hypersingular kernels – theory and applications to fracture mechanics. Int. J. Eng. Sci. 41, 683-720.
- Christian, J.W., Mahajan, S., 1995. Deformation twinning. Prog. Mater Sci. 39, 1-157.
- Chrysakis, A.C., Tsamasphyros, G., 1992. Numerical solution of integral equations with a logarithmic kernel by the method of arbitrary collocation points. Int. J. Numer. Meth. Eng. 33, 143-148.
- Cosserat, E., Cosserat, F., 1909. Théorie des corps déformables. Hermann et Fils, Paris.
- deWit, R., 1973. Theory of disclinations. IV. Straight disclinations. J. Res. N.B.S. A Phys. Ch. 77A, 608-658.
- Dundurs, J., Markenscoff, X., 1989. A Green's function formulation of anticracks and their interaction with load-induced singularities. J. Appl. Mech. 56, 550-555.
- Eshelby, J.D., 1951. The force on an elastic singularity. Phil. Trans. R. Soc. Lond. A 244, 87-112.
- Erdélyi, A., Magnus, W., Oberhettinger, F., Tricomi, F.G., Bateman, H., 1953. Higher transcendental functions. McGraw-Hill, New York.

- Fisher, B., 1971. The product of distributions. *Q. J. Math.* 22, 291-298.
- Freund, L.B., 1972. Energy flux into the tip of an extending crack in an elastic solid. *J. Elasticity* 2, 341-349.
- Gel'fand, I., Shilov, G., 1964. *Generalized Functions*, Vol. 1. Academic Press, New York.
- Georgiadis, H.G., 2003. The Mode III crack problem in microstructured solids governed by dipolar gradient elasticity: Static and dynamic analysis. *J. Appl. Mech.* 70, 517-530.
- Georgiadis, H.G., Velgaki, E.G., 2003. High-frequency Rayleigh waves in materials with micro-structure and couple-stress effects. *Int. J. Solids Struct.* 40, 2501-2520.
- Gourgiotis, P., Georgiadis, H., Sifnaiou, M., 2012. Couple-stress effects for the problem of a crack under concentrated shear loading. *Math. Mech. Solids* 17, 433-459.
- Gourgiotis, P., Piccolroaz, A., 2014. Steady-state propagation of a mode II crack in couple stress elasticity. *Int. J. Fract.* 188, 119-145.
- Gourgiotis, P.A., Georgiadis, H.G., 2007. Distributed dislocation approach for cracks in couple-stress elasticity: shear modes. *Int. J. Fract.* 147, 83-102.
- Gourgiotis, P.A., Georgiadis, H.G., 2008. An approach based on distributed dislocations and disclinations for crack problems in couple-stress elasticity. *Int. J. Solids Struct.* 45, 5521-5539.
- Gourgiotis, P.A., Georgiadis, H.G., 2009. Plane-strain crack problems in microstructured solids governed by dipolar gradient elasticity. *J. Mech. Phys. Solids* 57, 1898-1920.
- Grentzelou, C.G., Georgiadis, H.G., 2005. Uniqueness for plane crack problems in dipolar gradient elasticity and in couple-stress elasticity. *Int. J. Solids Struct.* 42, 6226-6244.
- Hills, D.A., Kelly, P.A., Dai, D.N., Korsunsky, A.M., 1996. *Solution of crack problems: the distributed dislocation technique*. Kluwer Academic Publishers.
- Huang, Y., Zhang, L., Guo, T.F., Hwang, K.C., 1997. Mixed mode near-tip fields for cracks in materials with strain-gradient effects. *J. Mech. Phys. Solids* 45, 439-465.
- Huang, Y., Chen, J.Y., Guo, T.F., Zhang, L., Hwang, K.C., 1999. Analytic and numerical studies on mode I and mode II fracture in elastic-plastic materials with strain gradient effects. *Int. J. Fract.* 100, 1-27.
- Itou, S., 1981. The effect of couple-stresses on the stress concentration around a moving crack. *Int. J. Math. Math. Sci.* 4, 165-180.

- Kobayashi, S., Ohr, S.M., 1981. In situ observations of the formation of plastic zone ahead of a crack-tip in copper. *Scripta Metall.* 15, 343-348.
- Koiter, W., 1964. Couple stresses in the theory of elasticity. Parts I and II, *Nederl. Akad. Wetensch. Proc. Ser. B*, pp. 17-29.
- Lubarda, V.A., 2003. The effects of couple stresses on dislocation strain energy. *Int. J. Solids Struct.* 40, 3807-3826.
- Lubarda, V.A., Markenscoff, X., 2000. Conservation integrals in couple stress elasticity. *J. Mech. Phys. Solids* 48, 553-564.
- Markenscoff, X., 1993. Interaction of dislocations and dislocation dipoles with cracks and anticracks. *Mater. Sci. Forum* 123, 525-530.
- Michot, G., George, A., 1986. Dislocation emission from cracks – observations by X-ray topography in silicon. *Scripta Metall.* 20, 1495-1500.
- Mindlin, R.D., 1964. Micro-structure in linear elasticity. *Arch. Ration. Mech. Anal.* 16, 51-78.
- Mindlin, R.D., Tiersten, H.F., 1962. Effects of couple-stresses in linear elasticity. *Arch. Ration. Mech. Anal.* 11, 415-448.
- Morini, L., Piccolroaz, A., Mishuris, G., 2014. Remarks on the energy release rate for an antiplane moving crack in couple stress elasticity. *Int. J. Solids Struct.*, 51 3087–3100.
- Ni, L., Markenscoff, X., 2008. The self-force and effective mass of a generally accelerating dislocation I: Screw dislocation. *J. Mech. Phys. Solids* 56, 1348-1379.
- Park, S.K., Gao, X.-L., 2006. Bernoulli-Euler beam model on a modified couple stress theory. *J. Micromech. Microeng.* 16, 2355-2359.
- Radi, E., 2008. On the effects of characteristic lengths in bending and torsion on Mode III crack in couple stress elasticity. *Int. J. Solids Struct.* 45, 3033-3058.
- Rice, J.R., Thomson, R., 1974. Ductile versus brittle behaviour of crystals. *Philos. Mag.* 29, 73-97.
- Roos, B.W., 1969. *Analytic functions and distributions in physics and engineering*. Wiley, New York.
- Sternberg, E., Muki, R., 1967. The effect of couple-stresses on the stress concentration around a crack. *Int. J. Solids Struct.* 3, 69-95.
- Tada, H., Paris, P., Irwin, G., 2000. *The analysis of cracks Handbook*. New York: ASME Press.

- Thomson, R., 1978. Brittle fracture in a ductile material with application to hydrogen embrittlement. *J. Mater. Sci.* 13, 128-142.
- Toupin, R.A., 1962. Perfectly elastic materials with couple stresses. *Archive of Rational Mechanics and Analysis* 11, 385–414.
- Vardoulakis, I., Sulem, J., 1995. *Bifurcation analysis in Geomechanics*. Blackie Academic & Professional, London.
- Weertman, J., 1978. Fracture mechanics: A unified view for Griffith-Irwin-Orowan cracks. *Acta Metall.* 26, 1731-1738.
- Zhang, T.-Y., Li, J.C.M., 1991. Image forces and shielding effects of an edge dislocation near a finite length crack. *Acta Metall. Mater.* 39, 2739-2744.